

Evidence for complete surface wave band gap in a piezoelectric phononic crystal

S. Benchabane, A. Khelif, J.-Y. Rauch, L. Robert, and V. Laude

Institut FEMTO-ST, CNRS UMR 6174, Université de Franche-Comté, F-25044 Besançon Cedex, France

(Received 10 February 2006; published 9 June 2006)

A complete surface acoustic wave band gap is found experimentally in a two-dimensional square-lattice piezoelectric phononic crystal etched in lithium niobate. Propagation in the phononic crystal is studied by direct generation and detection of surface waves using interdigital transducers. The complete band gap extends from 203 to 226 MHz, in good agreement with theoretical predictions. Near the upper edge of the complete band gap, it is observed that radiation to the bulk of the substrate dominates. This observation is explained by introducing the concept of the sound line.

DOI: [10.1103/PhysRevE.73.065601](https://doi.org/10.1103/PhysRevE.73.065601)

PACS number(s): 43.20.+g, 43.35.+d, 77.65.Dq

Phononic crystals ultimately offer control of the propagation of acoustic or elastic waves on a wavelength scale. Much like photonic crystals in the case of optical and electromagnetic waves, they consist of two- or three-dimensional periodic arrangements of two materials with differing elastic constants [1,2] that can give rise to absolute acoustic stop bands under well-chosen geometrical conditions. First demonstrations have generally been in the audible and ultrasonic range, with millimetric or larger wavelengths [3–8]. For instance, evanescent tunneling through a phononic crystal (PC) was observed [7], and guiding along and trapping of energy inside defects managed in a PC were demonstrated [9,10]. These theories and experiments have often been devoted to bulk acoustic waves (BAW's) for which the external boundaries enclosing the phononic crystal do not play a significant role in wave propagation. Yet, if phononic crystals have recently moved to the hypersonic region [11–13] and now appear as interesting candidates for high-frequency signal processing applications, the physical pathways to phononic devices still need to be defined. The case of surface acoustic waves (SAW's) has also attracted sustained attention [14–18]. SAW's are guided along the surface of a solid or liquid material and are hence confined in the direction normal to the surface. As a consequence, the two-dimensional periodic structuring of the surface can be expected to provide at least to a certain extent the same phononic properties for SAW's as would a three-dimensional phononic crystal for BAW's. This situation has a strong connection with the case of plasmonic crystals [19]. Phononic devices relying on surface waves in piezoelectric materials are attractive since SAW's can be directly excited and detected at the surface by use of interdigital transducers (IDT's) [20]. SAW-based components are extensively used as radio-frequency filters in wireless telecommunication systems; the integration of a phononic band gap structure to such devices would enhance their characteristics and widen their application range. From a fundamental point of view, piezoelectric phononic crystals enable experiments in which the sources and detectors of acoustic waves can be embedded with the phononic crystal itself, as shown in Fig. 1. The strong anisotropy of acoustic wave propagation inherent to piezoelectric materials, combined with the mixing of shear and longitudinal polarizations, strongly affect wave scattering. Yet it has been demonstrated theoretically that a complete band gap for SAW's, i.e., for any propagation direction of the impinging wave, can

be expected to exist [21] for a square lattice of holes in lithium niobate. A former experimental work has shown the existence of a directional stop band in a silicon phononic crystal, with a piezoelectric thin film ensuring surface wave transduction [22]. In this Rapid Communication, we report on the fabrication and experimental characterization of a complete band gap square-lattice SAW phononic crystal made of void inclusions etched in lithium niobate. The presented results open further prospects for designing a generation of phononic-crystal-based acoustic signal processing devices.

A finite element model was used to calculate the band diagrams for bulk waves propagating in the plane of the surface. Such a computation is sufficient for design purposes since it was observed that SAW and BAW band gaps coin-

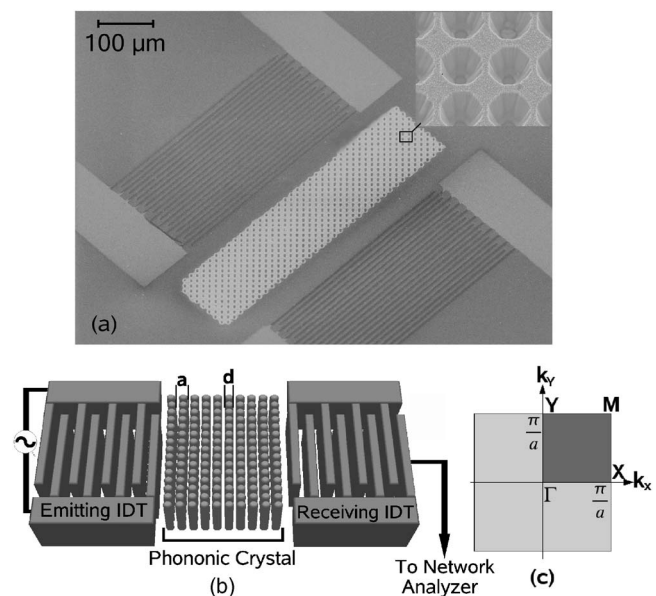


FIG. 1. (a) Scanning electron microscope image of a phononic crystal for surface acoustic waves. The structure, consisting of $9 \mu\text{m}$ diameter air holes with a $10 \mu\text{m}$ pitch, is surrounded by a pair of IDT's to ensure surface wave transduction. The inset in the top-right corner shows a more detailed view of the holes etched in the lithium niobate single crystal substrate. (b) Schematic of the experimental setup used for an electrical characterization of the crystal. (c) Sketch of the first Brillouin zone.

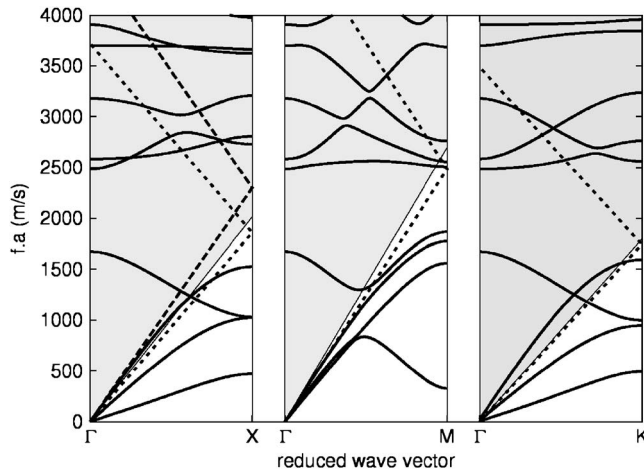


FIG. 2. Theoretical band diagrams for bulk waves propagating in the plane of a square lattice void/lithium niobate phononic crystal with a 64% filling fraction ($d/a=0.9$) along the ΓX , ΓM , and ΓY directions of the first Brillouin zone. In the grayed regions, above the sound lines, there is coupling of surface modes with the radiation modes of the substrate. The dispersion relations on a free surface are also indicated for the Rayleigh (short dashed line) and the leaky (long dashed line) surface waves. The theoretical band gap extends from 190 to 250 MHz when the lattice parameter a equals 10 μm .

cide [21], at least in the case of a square lattice of holes in a lithium niobate matrix. The phononic crystal is assumed to be infinite and arranged periodically along the surface. The whole domain is split into successive unit cells containing one hole surrounded with the matrix material. The unit cell is meshed and divided into elements connected by nodes. Bloch-Floquet periodic boundary conditions are applied at the boundaries of the unit cell. Considering a time-harmonic variation of all fields with a time dependence $\exp(i\omega t)$, where ω is the angular frequency, the general piezoelectric problem with no external applied force is written as

$$\begin{bmatrix} K_{uu} - \omega^2 M_{uu} & K_{u\phi} \\ K_{\phi u} & K_{\phi\phi} \end{bmatrix} \begin{pmatrix} u \\ \phi \end{pmatrix} = \begin{pmatrix} 0 \\ 0 \end{pmatrix} \quad (1)$$

where K_{uu} and M_{uu} are the stiffness and mass matrices of the purely elastic part of the problem, $K_{u\phi}$ and $K_{\phi u}$ are piezoelectric-coupling matrices, and $K_{\phi\phi}$ is the purely dielectric part. u and ϕ , are, respectively, the nodal displacements and electrical potential. As the angular frequency is a periodical function of the Bloch-Floquet wave vector, the band diagram is obtained by solving an eigenvalue problem inside the first irreducible Brillouin zone. In an anisotropic and piezoelectric material such as lithium niobate [23], numerical simulations for a square lattice of holes predict a complete band gap width as large as 34% for a 64% filling fraction, as shown in Fig. 2. The diameter over pitch (d/a) ratio of the structure, as defined in Fig. 1, is then around 0.9. Figure 2 displays the band diagrams for the ΓX , ΓM , and ΓY propagation directions. These directions encompass the main points of symmetry of the first Brillouin zone, and are the relevant directions to consider for an experimental investiga-

tion of an anisotropic phononic structure. Although crystals with lower d/a values would certainly prove easier to fabricate, the way the complete band gap width scales with the filling fraction of the structure does not really allow for a large margin. The band gap width tends to rapidly decrease and is eventually reduced to zero when the filling fraction is below 50%, that is for a diameter over pitch ratio below 0.8.

The phononic crystal in Fig. 1 was fabricated on a 500 μm thick, Y-cut lithium niobate wafer. This cut was chosen because of its particularly strong piezoelectric coefficients and low acoustic losses. However, the fabrication process is relatively insensitive to this parameter. The principal axes of the square-lattice phononic crystal are aligned with the crystallographic X and Z axes. To be able to use optical lithography and plain reactive ion etching (RIE) for the patterning of the phononic structure, we have chosen to work at a center frequency of 200 MHz. This, in accordance with numerical simulations, sets a lattice parameter of 10 μm and a hole diameter around 9 μm , leading to a forbidden complete band gap running from 190 to 250 MHz. Holes were machined using standard sulfur-hexafluoride-based RIE at low pressure (around 2 μbar) and high power (200 W). The etching rate is very low, around 50 nm min^{-1} , and the etching slope is quite significant (around 17% for a 10 μm diameter hole). This limits the depth and aspect ratio, but also the achievable hole diameters, as we observed that the etching slope increases as the hole diameter decreases. A highly selective, 1 μm thick electroplated nickel mask enables us to obtain relatively satisfying 10 μm deep holes. The finite element model used does not take either the conicity of these holes, or their finite depth into account. However, the penetration depth of Rayleigh-type SAW's in the substrate is approximately one wavelength. We then expect the crystal to be deep enough to allow for a significant band gap effect.

Brillouin light scattering was used by Gorishnyy *et al.* to retrieve the full band diagram for elastic modes [11]. Since we wish to demonstrate a complete band gap, we have opted for transmission measurements of these finite size phononic crystals. The fabrication of a sequence of IDT's, on the substrate surface allowed for the direct electrical excitation and detection of SAW's traveling through the PC. A large measurement frequency range, from 150 to 300 MHz, was chosen in order to cover the complete band gap. Singly periodic interdigital transducers do not allow such a wide bandwidth to be covered at once, as they are limited by the available piezoelectric coupling, less than 5% with Y-cut lithium niobate. To overcome this problem, Wu *et al.* employed fan-shaped IDT's [22]. However this approach is not usable here, as we argue later. Alternatively, we used a series of eight ten-finger-pair IDT's of varying mechanical period, corresponding to emission wavelengths ranging from 12.2 to 26 μm . The frequency range of interest is then covered by juxtaposing neighboring responses. IDT's were realized by patterning a 150 nm thick aluminum layer, and were oriented for elastic wave propagation along the ΓX , ΓM , and ΓY directions of the first Brillouin zone. Two series of test structures were fabricated, with and without a phononic crystal in between the transmitting and the receiving IDT's, respectively. The structures without a phononic crystal were used as references.

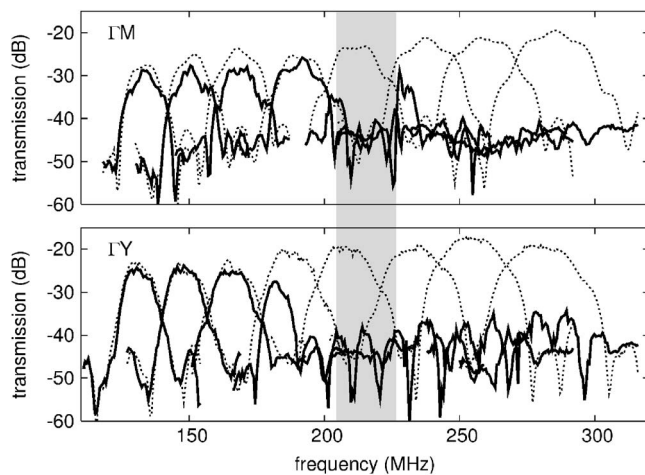


FIG. 3. Measurements of the eight reference devices (dotted line) and the eight phononic band gap devices (solid line) along the ΓM and ΓY directions.

The electrical transmission was measured using a network analyzer. Figure 3 displays the transmission spectra for both the reference and the phononic crystal devices measured along the ΓY and the ΓM directions. These measurements clearly show that at frequencies below 180 MHz along ΓY , and below 200 MHz along ΓM , the reference and crystal signals almost perfectly overlap; the Rayleigh wave propagation is not affected by the presence of the crystal. Above these frequencies, the transmitted signal experiences a strong attenuation, with losses estimated to be around 20 dB for a ten-period-long crystal. Surprisingly, there is no increase in transmission at frequencies higher than 230 MHz, as would be expected from the band diagram in Fig. 2. The signal does not recover at all along ΓY , and only a rather narrow transmission peak—about 5 MHz large—around 230 MHz is observed along ΓM . Any higher-frequency mode propagating in the structure seems to be inhibited.

Similar results are observed along the ΓX direction. Let us notice, however, that, in the case of Y-cut lithium niobate, in addition to the pure Rayleigh SAW aimed at, a leaky SAW also exists in the homogeneous half space, though its range of existence is limited to angles around the X crystallographic axis [21]. This transversally polarized leaky SAW has limited attenuation and penetrates far deeper in the substrate than the Rayleigh SAW does, typically for several tens of wavelengths. Because of the limited depth of the holes, it is expected to experience the substrate periodicity in a less significant way than the Rayleigh SAW. The leaky SAW velocity is close to that of the Rayleigh SAW (4600 versus 3700 m s^{-1}), which leads to an overlap of their electrical responses in measurements. This makes the use of wide bandwidth fan-shaped IDT's ambiguous. Thus, for a better readability, Fig. 4 presents measurements for only four out of the eight IDT's, although all of them were measured. The corresponding devices have an emission wavelength of 26, 20.6, 16.4, and $14.6 \mu\text{m}$, respectively. For these emission wavelengths, the Rayleigh and the leaky SAW's are successively before, inside, and after the band gap, theoretically extending from 190 to 250 MHz. The Rayleigh SAW shows

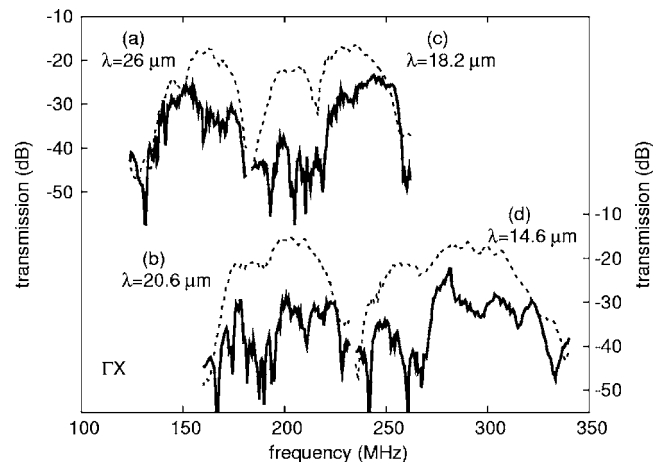


FIG. 4. Measurements of four reference devices (dotted line) and four phononic band gap devices (solid line) along the ΓX direction. Both the Rayleigh and the leaky surface waves exist simultaneously and give rise to adjacent frequency responses.

the same behavior as in the other two directions; it remains almost unaltered below the band gap, but experiences the same sharp 20 dB attenuation inside it. Here again, there is no significant increase in transmission at frequencies higher than the theoretically predicted upper gap frequency. Conversely, the leaky SAW always suffers an attenuation of approximately 10 dB, seemingly irrespective of the presence of the band gap.

Figure 5 gives a summary of the measurements for the Rayleigh SAW. The relative transmission is computed as the ratio of the transmittances with and without the phononic crystal. If a full band gap has definitely opened, with the crystal causing a 20 dB loss in the transmission value for pure surface modes, the upper edge of the full band gap is not clearly apparent. To account for this phenomenon, let us come back to the fact that the actual crystal is not the ideal, two-dimensional phononic crystal considered in our theory. Since the surface wave penetration depth in the substrate remains of the same order as the hole depth, the actual phononic crystal can then be seen as a stratified medium,

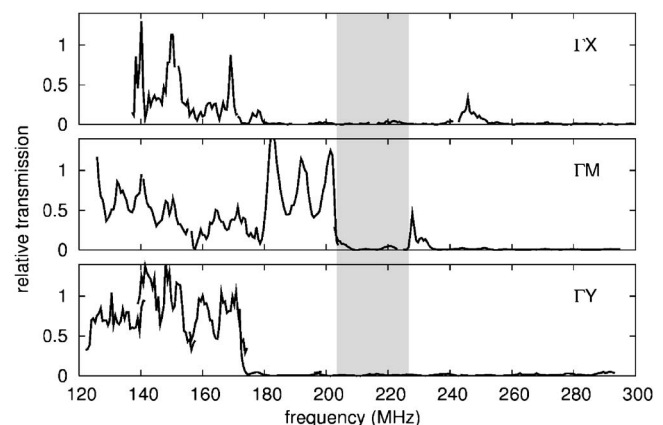


FIG. 5. Relative transmission, defined as the ratio of the transmittances with and without a phononic crystal. The complete band gap extends from 203 to 226 MHz.

with a void/lithium niobate phononic crystal slab lying atop bulk lithium niobate. This, combined with the conicity of the holes tends to favor out-of-plane scattering, leading to coupling with bulk modes of the substrate. To tackle this problem, we use an analogy with 2.5-dimensional (2.5D) photonic crystals [24]. These generally consist of a 2D photonic crystal etched through a high-index guiding layer on a lower-index substrate. Guided modes as well as radiation modes into the substrate are expected to exist, and the limit between these modes is set by the light line in the substrate. The *sound line* can be defined as the dispersion relation of the slowest bulk acoustic mode in the substrate. The corresponding *sound cones* were superimposed on the band diagrams in Fig. 2. Surface modes lying inside the sound cone are, possibly, highly lossy, radiation modes. Only modes below the sound line are guaranteed to be guided by the surface, which agrees well with the experimental results. In the case of the Rayleigh SAW, this argument accounts for both the extinction of the signal at high frequencies along the ΓX and ΓY directions, and also for the peak observed along ΓM which

corresponds to modes belonging to the upper part of the band diagram but still lying below this line. The leaky SAW being always faster than the slowest shear bulk wave, it is always above the sound line, and hence always experiences strong radiation to the interior of the substrate, again in agreement with the experimental observations.

In conclusion, we have investigated elastic band gaps for surface waves in a phononic crystal etched in lithium niobate. The crystal has been characterized electrically by direct piezoelectric generation and detection of SAW's. A full band gap has been found, in close agreement with theory. The concept of a sound line was used to explain the apparent vanishing of surface waves at higher frequencies. These promising results open additional prospects for phononic devices exploiting phononic band gap properties.

We gratefully acknowledge the help of V. Pétrini and W. Daniau for device preparation, and of Th. Pastureaud for SAW simulation. This work was supported by the ACI "Nanosciences" under Grant No. 137/2004.

-
- [1] M. Sigalas and E. Economou, *Solid State Commun.* **86**, 141 (1993).
 - [2] M. S. Kushwaha, P. Halevi, L. Dobrzynski, and B. Djafari-Rouhani, *Phys. Rev. Lett.* **71**, 2022 (1993).
 - [3] E. N. Economou and M. Sigalas, *J. Acoust. Soc. Am.* **95**, 1734 (1994).
 - [4] F. R. Montero de Espinosa, E. Jiménez, and M. Torres, *Phys. Rev. Lett.* **80**, 1208 (1998).
 - [5] J. V. Sánchez-Pérez, D. Caballero, R. Martínez-Sala, C. Rubio, J. Sánchez-Dehesa, F. Meseguer, J. Llinares, and F. Gálvez, *Phys. Rev. Lett.* **80**, 5325 (1998).
 - [6] D. García-Pablos, M. Sigalas, F. R. Montero de Espinosa, M. Torres, M. Kafesaki, and N. García, *Phys. Rev. Lett.* **84**, 4349 (2000).
 - [7] S. Yang, J. H. Page, Z. Liu, M. L. Cowan, C. T. Chan, and P. Sheng, *Phys. Rev. Lett.* **88**, 104301 (2002).
 - [8] S. Yang, J. H. Page, Z. Liu, M. L. Cowan, C. T. Chan, and P. Sheng, *Phys. Rev. Lett.* **93**, 024301 (2004).
 - [9] M. Torres, F. R. Montero de Espinosa, D. García-Pablos, and N. García, *Phys. Rev. Lett.* **82**, 3054 (1999).
 - [10] A. Khelif, A. Choujaa, B. Djafari-Rouhani, M. Wilm, S. Balandras, and V. Laude, *Phys. Rev. B* **68**, 214301 (2003).
 - [11] T. Gorishnyy, C. K. Ullal, M. Maldovan, G. Fytas, and E. L. Thomas, *Phys. Rev. Lett.* **94**, 115501 (2005).
 - [12] B. Bonello, A. Ajinou, V. Richard, P. Djemia, and S. M. Chérif, *J. Acoust. Soc. Am.* **110**, 1943 (2001).
 - [13] D. H. Hurley and K. L. Telschow, *Phys. Rev. B* **66**, 153301 (2002).
 - [14] T. Aono and S.-I. Tamura, *Phys. Rev. B* **58**, 4838 (1998).
 - [15] Y. Tanaka and S. I. Tamura, *Phys. Rev. B* **60**, 13294 (1999).
 - [16] R. E. Vines, J. P. Wolfe, and A. V. Every, *Phys. Rev. B* **60**, 11871 (1999).
 - [17] F. Meseguer, M. Holgado, D. Caballero, N. Benaches, J. Sánchez-Dehesa, C. López, and J. Llinares, *Phys. Rev. B* **59**, 12169 (1999).
 - [18] T.-T. Wu, Z.-C. Hsu, and Z.-G. Huang, *Phys. Rev. B* **71**, 064303 (2005).
 - [19] S. C. Kitson, W. L. Barnes, and J. R. Sambles, *Phys. Rev. Lett.* **77**, 2670 (1996).
 - [20] R. M. White and F. W. Voltmer, *Appl. Phys. Lett.* **17**, 314 (1965).
 - [21] V. Laude, M. Wilm, S. Benchabane, and A. Khelif, *Phys. Rev. E* **71**, 036607 (2005).
 - [22] T. Wu, L. Wu, and Z. Huang, *J. Appl. Phys.* **97**, 094916 (2005).
 - [23] G. Kovacs, M. Anhorn, H. E. Engan, G. Visintini, and C. C. W. Ruppel, *Proc.-IEEE Ultrason. Symp.* **1**, 435 (1990).
 - [24] J. Joannopoulos, R. Meade, and J. Winn, *Photonic Crystals* (Princeton University Press, Princeton, NJ, 1995).